

Optimising Electric Vehicle Charging Station Placement using Advanced Discrete Choice Models

Steven Lamontagne¹, Margarida Carvalho¹, Emma Frejinger¹, Bernard Gendron¹,
Miguel F. Anjos², and Ribal Atallah³

¹CIRRELT and Département d’informatique et de recherche opérationnelle,
Université de Montréal

²School of Mathematics, University of Edinburgh

³Institut de Recherche d’Hydro-Québec

June 23, 2022

1 Introduction

In order to meet CO₂ emissions goals, major changes at the global level are necessary. This includes the transportation sector, which in 2019 was responsible for 27% of global CO₂ emissions (International Energy Agency 2021) and 30% of emissions in Canada (Environment and Climate Change Canada 2021). One initiative that has been proposed to reduce these emissions is the adoption of electric vehicles (EVs), rather than internal combustion engine vehicles (ICEVs). Depending on the electricity generation mix, this may be effective in reducing emissions (Axsen et al. 2015a, Woo et al. 2017).

Due to the limits of the internal battery, EVs require more frequent refuelling than CVs. While early adopters of EVs may have access to home charging (Bailey et al. 2015), this can be supplemented with public charging infrastructure to increase accessibility. The availability of the latter has been found to increase EV adoption (e.g. Coffman et al. 2017). However, this scenario has been noted to suffer from a “chicken-and-egg” dilemma (Anjos et al. 2020), where users require charging infrastructure in order to purchase an EV, while businesses and infrastructure operators have little incentive to install charging stations when there are few users. To this end, governmental organisations can alleviate this problem by investing in public charging infrastructure, thus allowing users to recharge EVs and encourage EV adoption.

The problem we examine is that of the decision makers responsible for public charging infrastructure, and the optimal placement of that infrastructure within a city. They have a set of candidate locations for charging stations, and must decide which charging stations to open as well as how many charging outlets to place at each open station. These decisions

take place over a long-term planning horizon, and investment in each period is limited by a budget. The decision makers take into account the users who are purchasing a vehicle in each period. Depending on the placement of charging infrastructure, these users may purchase an EV. We assume that the users anticipate the need to recharge an EV, and will only purchase one if they have access to charging infrastructure (either public or at home). Additionally, we assume that more convenient charging (e.g. by a charging station being closer to home, or having more charging outlets) increases the probability that a user will purchase an EV. The goal of the decision makers is to plan the placement of charging infrastructure so that it maximises EV adoption.

The existing literature for this problem is quite narrow, and has limitations that we address in this work. In the intercity context, the optimisation model of Zhang et al. (2017) accounts for EV adoption growth depending on the coverage of paths, but their method is not applicable to the intracity case. To the best of our knowledge, in the intracity context, only Anjos et al. (2020) formulate an optimisation model for locating charging stations accounting for EV adoption growth based on the location of charging stations. There, the total number of EVs increases according to a piecewise-linear growth function, which accounts for natural growth. This growth function is applied indiscriminately to all locations. Additionally, the fraction of users who have access to home charging is assumed to be constant across locations in the network. In reality, the EV growth rate varies by location (Association des Véhicules Électrique du Québec 2021), and access to home charging depends on the type of residences (Nicholas et al. 2019).

This work presents modelling, algorithmic, and computational contributions. For the modelling side, we consider user classes, allowing for parameter values to be considered more specifically for groups of users rather than the entire population. Additionally, within each user class, the optimisation model supports the use of advanced discrete choice models. This allows to model heterogeneous user preferences and complex substitution patterns. The combination of the user classes and the ability to use advanced discrete choice models results in a highly flexible model, which the decision makers can design to suit their specific problem and available data sources. The user behaviour is incorporated in the decision-maker’s problem as in Pacheco Paneque et al. (2021), leading to a bilevel program. While the bilevel optimisation model presented here can only solve small instances, the maximum covering reformulation allows for instances to be solved significantly faster. This reformulation is effective for our optimisation model, but is also applicable to more general, uncapacitated bilevel models using the framework of Pacheco Paneque et al. (2021). On the algorithmic side, we propose three heuristics to solve the optimisation models. The first heuristic is a rolling horizon method, which was also used in Anjos et al. (2020). We also present a greedy method (Church and ReVelle 1974) and a GRASP method (Resende 1998), which we extend to a multi-period setting with sizing decisions. On the computational side, we present extensive experiments both to compare the capabilities of our optimisation model with the model presented in Anjos et al. (2020) and to compare the heuristic methods. Where possible, parameter values and user class characteristics are based on real data.

Section 2 reviews the relevant literature for the problem. Section 3 describes the framework of the problem. Section 4 describes the upper and lower-level problems, and it additionally provides the complete stochastic, bilevel optimisation model. Section 5 gives the maximum covering reformulation for the bilevel model. Section 6 discusses various heuristic methods for solving larger instance sizes. Section 7 provides computational results, comparing the capabilities of the maximum covering formulation against the model in Anjos et al. (2020), and comparing the heuristics methods presented in Section 6.

2 Literature Review

We review three topics of research that relate closely to our work. The first topic is that of EV charging station location models, which determines the optimal location for charging stations. The second topic is that of vehicle acquisition, more specifically relating to EVs, which discusses factors that affect whether users purchase EVs. The third topic is that of the Maximum Capture Problem with Random Utilities (MCPRU), which examines the optimal placement of facilities in a competitive environment.

On the topic of EV charging station location models, the model proposed by Anjos et al. (2020), which we refer to as the *Growth Function model*, is the closest to our work. Whereas most charging station location models are examined with the objective to maximise profits or minimise costs, the Growth Function model is designed solely to encourage electric vehicle adoption. Its use of a combination of node-based and path-based approaches allows for the inclusion of a general highway charging station network while allowing for increased precision within the city. EV adoption and charging stations are linked via capacity constraints, with users willing to recharge at any charging station within a fixed distance of their home.

There is an existing literature for EV charging station placement (an excellent review is presented in Kadri et al. 2020), however two notable differences separate it from our work. First, in all cases, the users under consideration are those who already own EVs, and are deciding on a charging station to recharge. Second, the objective of the decision maker are different, such as profit maximisation (Luo et al. 2015), maximising the EV flow that can travel each path given a limited EV range (Lim and Kuby 2010), minimising the users' costs for recharging the EV and travel time (González et al. 2022), or maximising the EV charging demand that can be covered (Frade et al. 2011). We provide a summary of the key characteristics of related works in Table 1.

Estimation of the EV recharging demand at each station or along each path is generally taken to be deterministic. However, in Luo et al. (2015) and Cui et al. (2019) the demand for each station is estimated using the analytic choice probabilities from a nested logit model. The demand model they use considers station characteristics such as the distance to the EV owner and the proximity of the charging station to amenities (such as restaurants and shopping centres). In Kadri et al. (2020), the evolution each year of the demand for each path is modelled with a discrete scenario tree. In the tree, the demand for the current year

is assumed to be known, as are the transition probabilities for each of the possible states in each subsequent year. This allows for the estimation of the expected demand of each path considering all subsequent years.

The inclusion of capacity constraints in EV charging station location models is not consistent. Several models (including our work, as well as others in Table 1) do not consider capacity. For those that do include capacity constraints, the modelling assumptions may differ. In Frade et al. (2011) and Zhang et al. (2017), the demand that may be satisfied by each charging station is limited by the number of outlets installed at that location. In Luo et al. (2015), the decision maker must ensure that charging stations meet minimum quality of service requirements, including waiting time and service coverage. In Cui et al. (2019), the decision maker must ensure that the amount of electricity supplied at each charging station is sufficient for the expected amount of demand. In González et al. (2022), the number of recharging sessions that will be required at each station is estimated, and used as a bound for the capacity of the station.

The vehicle acquisition problem examines the factors that increase the likelihood of purchasing EVs, and are useful for determining exogenous factors for the demand model and defining the classes of users. A key factor that has been examined is the core principle of our model: the availability of electric vehicle charging stations increases the likelihood of users purchasing an EV. Of the articles that examine the prevalence of charging stations (also referred to as ‘fuel availability’), most found that it was a significant factor in the decision to purchase an EV (Achtnicht et al. 2012, Javid and Nejat 2017, Hackbarth and Madlener 2013, Ziegler 2012, Rezvani et al. 2015, Coffman et al. 2017). This finding is not unanimous however, as Bailey et al. (2015) propose that a predisposition to EVs makes the users more likely to notice existing charging infrastructure, not the converse. The conclusions of Bailey et al. (2015) are also present in Axsen et al. (2015b), an article based on the same dataset and project.

Though the importance of public charging infrastructure is crucial for the demand model, many more factors have been considered for EV adoption and associated parameter values have been estimated using discrete choice models. Heterogeneity within the population, a foundation for discrete choice models, can be observed even in the latent class models of Hidrue et al. (2011) and Axsen et al. (2015b). Some examples of factors include the purchase price of EVs, the fuel costs for EVs or ICEVs, environmental awareness, age, gender, income, home charging access, and education (Hidrue et al. 2011, Achtnicht et al. 2012, Ziegler 2012, Hackbarth and Madlener 2013, Axsen et al. 2015b, Bailey et al. 2015, Javid and Nejat 2017). For reviews of EV acquisition models, we refer to Rezvani et al. (2015), Javid and Nejat (2017), and Coffman et al. (2017).

In this work, we formulate the problem as a MCPRU, generally attributed to Benati (1999) and Benati and Hansen (2002). In the MCPRU, a company is looking to place facilities in an environment where competitors have existing facilities. A *Random Utility Maximisation* (RUM) model is used to predict the choice of the users, based on the set of facilities available to them. The company aims to place the new facilities to maximise the market share that

	Objective	Model Type	Demand	Time Periods	Capacity	Intracity or Intercity
Lim and Kuby (2010)	Maximise flow refueled	FRLM	D	Single	No	Inter
Frade et al. (2011)	Maximise coverage of EV charging demand	Maximum Covering	D	Single	Yes	Intra
Shukla et al. (2011)	Maximise flow intercepted	FILM	D	Single	No	Intra
Capar et al. (2013)	Maximise flow refueled	FRLM	D	Single	No	Inter
Luo et al. (2015)	Maximise profit of decision maker	MINLP	S	Multi	Yes	Intra
Zhang et al. (2017)	Maximise flow refueled	FRLM	D	Multi	Yes	Inter
Cui et al. (2019)	Minimise cost of decision maker	MINLP	S	Multi	Yes	Intra
Badri-Koohi et al. (2019)	Minimise costs, p-median, flow interception (weighted sum)	MILP	D	Single	No	Intra
Kadri et al. (2020)	Maximise flow refueled	FRLM	S	Multi	No	Inter
González et al. (2022)	Minimise users' travel cost	Bilevel	D	Single	Yes	Intra

Legend: FRLM = Flow Refueling Location Model, FILM = Flow Interception Location Model, MINLP = Mixed Integer Non-Linear Problem, MILP = Mixed Integer Linear Problem, D = Deterministic, S = Stochastic.

Table 1: Summary of key characteristics of EV charging station location models.

the new facilities capture. In general, the MCPRU focuses on two key attributes of facilities in order to determine which one users choose to patronise: distance to the users, and *facility attractiveness* (Berman et al. 2014). It is possible to consider market expansion in the MCPRU, where the placement of facilities attracts customers that were not originally in the market (see, e.g., Aboolian et al. 2007). Since a vehicle (EV or otherwise) is an expensive purchase, it is assumed that the additions to the charging infrastructure are not sufficient to attract users who were not planning on purchasing a vehicle at all in the given period. We thus do not include market expansion in our optimisation model.

Almost all work on the MCPRU has been done in the context of using the multinomial logit model for characterising user behaviours, due to the existence of an analytic formula for calculating choice probabilities. For recent examples, the linear formulation in Freire et al. (2016) (which improves on the linear formulation in Haase 2009) and the outer approximation and submodular cut methods in Ljubić and Moreno (2018) both rely on the logit choice probabilities. Exceptions to the use of multinomial logit include the work of Mai and Lodi (2020), who express a mixed logit choice probability as a sum of probabilities of multinomial logit models (though they do not conduct any computational experiments using this method), and the work of Dam et al. (2021), who use a method that makes use of the submodularity of the objective function for all discrete choice models in the Generalised Extreme Value (GEV) family (of which multinomial logit and mixed logit are included). Since we do not assume the use of multinomial logit or the GEV family (in addition to the added complexity of multi-period and sizing considerations), the methods proposed in these works cannot be applied directly to our model.

While it can be used more generally, the simulation-based approach in Pacheco Paneque et al. (2021) can be applied to the MCPRU. Rather than embedding an analytic probability that users will select an alternative into the objective function, this approach instead generates error terms for each alternative for a given number of *scenarios*. These error terms, pre-computed and given to the optimisation model as an input, allow for the utility to be calculated for each alternative and each scenario. Using the principle of Random Utility Maximisation (RUM), users then select, in each scenario, the alternative which has the highest utility. Alternatives which are not available to users (such as, in the case of the MCPRU, facilities which are closed) are set to a lower bound, ensuring they are not selected. Since this approach relies upon pre-computed error terms, it supports the use of any discrete choice model rather than being limited to the multinomial logit model (or even the GEV family). However, this results in a model which is computationally difficult to solve in larger instances.

Our work aims to bridge the gap between the EV charging station placement models, EV acquisition models, and the MCPRU. Most EV charging station placement models are designed to benefit existing EV owners, instead of maximising EV adoption. The existing works which include EV growth based on the placement of EV charging stations, namely the models of Zhang et al. (2017) and Anjos et al. (2020), use an aggregate approach for EV growth. However, the literature on EV acquisition shows that significant factors for determining EV acquisition are individual characteristics of the users (e.g. income, education

level, access to home charging). This highlights the benefit of user classes in our optimisation model, as they allow for these individual characteristics to be considered. Moreover, we note the heterogeneity within each preference class (which function equivalently as a user class in our work) in the latent class models of Hidrue et al. (2011) and Aksen et al. (2015b). This suggests the use of a discrete choice model for demand modelling, and naturally leads to a MCPRU formulation for the optimisation model. As is the case for the MCPRU, in addition to user characteristics, characteristics from the charging station also impact the choice of users. While the specification of the discrete choice model for the users is outside the scope of this work, we will note later characteristics of the demand modelling which makes the multinomial logit model less suitable. Because of this, we use the simulation-based approach of Pacheco Paneque et al. (2021), which allows for any discrete choice model to be used.

3 Problem Formulation

In our problem, we consider the placement of charging infrastructure in a city, wherein there are two parties with different motives: a decision maker placing public EV charging infrastructure, and the users choosing whether to purchase an EV (depending on the charging infrastructure). An illustration of this process is given in Figure 1.

3.1 Decision Maker

The decision maker is planning charging infrastructure over a planning horizon with T periods (e.g., seasons or years) indexed by $1 \leq t \leq T$. The decision maker has a candidate set of locations M where charging stations $j \in M$ may be installed or expanded with additional outlets to a maximum number m_j . In each period t , there is a budget B^t , which limits the total investment (both opening stations and installing outlets). Let f_j^t and c_j^t denote, respectively, the cost to open the station and to install an outlet at charging station $j \in M$ in period t .

Let y_j^t be a binary variable indicating if station $j \in M$ is open in period t , and let x_{jk}^t be a binary variable indicating if station $j \in M$ has k outlets in period t (with $1 \leq k \leq m_j$). We denote $\mathbf{x} = \{x_{jk}^t\}$ and $\mathbf{y} = \{y_j^t\}$ with $j \in M, 1 \leq k \leq m_j, 1 \leq t \leq T$. Let x_j^0 and y_j^0 denote the initial state of each charging station j , respectively, the number of outlets and whether the station is open.

3.2 Users

The users are planning on purchasing a vehicle and, depending on public charging infrastructure, may choose to purchase an EV. These users are composed of a set of user classes N . The population size for each user class is given by $N_i^t, i \in N, 1 \leq t \leq T$.

Each user considers whether they have a primary option for recharging an EV. If such an option is available and sufficient for their needs, they decide to purchase an EV. This decision

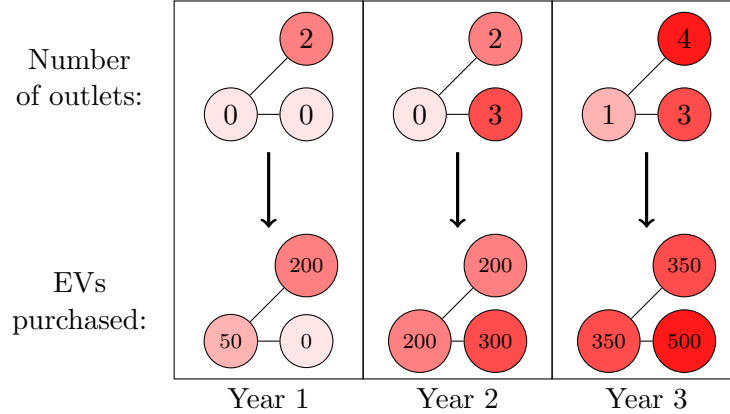


Figure 1: The decision maker decides where to place charging infrastructure (stations and number of outlets) on the simple example network. In response, a subset of users decide to purchase EVs.

is modelled via a discrete choice model, with users in user class $i \in N$ selecting an alternative j in choice set $\mathcal{C}_i^t(\mathbf{y})$. The inclusion of \mathbf{y} in the notation for the choice set emphasises the dependence on the set of open stations, since stations which are closed cannot be used to recharge an EV. The choice set $\mathcal{C}_i^t(\mathbf{y})$ contains a subset of the public charging infrastructure, home charging (if available to user class i), and an opt-out. The latter corresponds to the alternative to not purchase an EV, while all other alternatives indicate the user purchases one. In what follows, we denote the opt-out alternative as $j = 0$.

Each charging station $j \in M$ that is opened is assumed to be *uncapacitated*, in the sense that there is no limit to the number of users that may select it. However, we assume that the likelihood of users selecting a given station increases with the number of outlets. The rationale being that the higher the number of outlets, the more likely one may be available when required. This allows us to implicitly take into account that users perceive the capacity as finite.

The natural hierarchical structure of the problem suggests a bilevel formulation, with the decision maker in the upper-level and the users in the lower-level. The choice in the lower-level to purchase an EV is modelled via a discrete choice model.

4 Bilevel Optimisation Model

Bilevel optimisation models sequential decision making, where first, the leader takes a decision (*upper level*) and then, the followers react by solving an optimisation problem (*lower level*). The optimal solution of a bilevel model are the decision values for the leader that optimise its objective function, based on the optimal reaction of the lower-level users to the values of those variables.

The followers in this case are the users, whose optimisation problem maximises their *utility*. More specifically, the users must choose an alternative from a finite set of available alternatives (here, open stations, home charging, and opt-out). The value of each alternative is predicted through the use of a *utility function*, which associates the value of a given alternative for users based on observable and unobservable factors. Under the assumption of *utility maximisation*, users then, as rational beings, select the alternative which presents the maximum benefit to them, as represented by the alternative with the highest utility. For each period $1 \leq t \leq T$, user class $i \in N$, and alternative $j \in C_i^t(\mathbf{y})$, the utility is denoted u_{ji}^t .

The analyst has imperfect knowledge of the utility of the users, so we model it as a random variable. Hence, instead of a deterministic model identifying the alternative chosen by the users, we obtain a probability distribution over the set of available alternatives. Consequently, the leader maximises the expected number of users purchasing an EV or, equivalently, minimises the expected number of users that *do not* purchase an EV. This is given by

$$\min_{(x,y) \in X} \sum_{t=1}^T \sum_{i \in N} N_i^t \mathbb{P}_\varepsilon [u_{0i}^t(x, \varepsilon) \geq u_{ji}^t(x, \varepsilon), \forall j \in C_i^t(y)], \quad (1)$$

where X denotes the upper-level constraints, and ε denotes the random error term. These constraints are discussed in more detail in Section 4.2. We recall that index $j = 0$ indicates the opt-out alternative, thus u_{0i}^t is the opt-out utility for user class i in year t .

If the error terms are independent, and identically extreme-value type I distributed, the choice probabilities have an analytic formula (the well-known multinomial logit model). In our application, this assumption may not hold. For example, if stations are near each other, they will also have similar amenities near them (e.g. restaurants, shopping centres, etc.). If a user places high value in those amenities (and they are not explicitly included in the observable factors), the error terms for those stations may be highly correlated. To allow for general discrete choice models which relax this restriction and support flexible substitution patterns, we use the simulation-based approach of Pacheco Paneque et al. (2021).

Let R_i be the number of *scenarios* for user class i , and let ε_{ji}^{rt} denote the realisation of the random variable ε for user class i , alternative j , scenario r , and period t . Then, $\forall j \in C_i^t(y)$, we denote

$$w_{ji}^{rt} = \begin{cases} 1, & \text{if } j = \arg \max_{j' \in C_i^t(y)} \{u_{j'i}^t(x, \varepsilon_{j'i}^{rt})\}, \\ 0, & \text{otherwise.} \end{cases} \quad (2)$$

The details of the lower-level problem are discussed in Section 4.1. For the sake of simplicity, in a flagrant abuse of notation, we denote the vector $\mathbf{w} = \{w_{ji}^{rt}\}$ with w_{ji}^{rt} given by (2) for each $i \in N, 1 \leq t \leq T, 1 \leq r \leq R_i, j \in C_i^t(y)$ as $\mathbf{w} \in \arg \max_{j \in C(y)} \{u(x, \varepsilon)\}$. Then, we can

write a sample average approximation of (1) as

$$\begin{aligned} \min_{(x,y) \in X} & \sum_{t=1}^T \sum_{i \in N} N_i^t \frac{1}{R_i} \sum_{r=1}^{R_i} w_{0i}^{rt}, \\ \text{s.t. } \mathbf{w} &= \arg \max_{j \in C(y)} \{u(x, \varepsilon)\}. \end{aligned}$$

4.1 Lower-Level Problem

The lower-level problem is assumed to be separable for each user class, each period, and each scenario, meaning that there is no interaction among them. Therefore, in what follows, we concentrate on detailing user class $i \in N$ in scenario $1 \leq r \leq R_i$ at period $1 \leq t \leq T$. For each alternative $j \in C_i^t(\mathbf{y})$, let $u_{ji}^{rt} = u_{ji}^t(x, \varepsilon_{ji}^{rt})$ be the *simulated utility*.

We previously remarked that the choice set $C_i^t(\mathbf{y})$ depends on which stations are open. For notational simplicity, we define the two choice sets: C_i^{0t} and C_i^{1t} .

The set C_i^{0t} includes all alternatives exogenous to the optimisation model (i.e. unaffected by decision variables), for which the availability is not under the control of the decision maker. This always includes the opt-out alternative, but may also, for example, include the alternative for home charging. The simulated utility u_{ji}^{rt} , for $j \in C_i^{0t}$, is thus given by

$$u_{ji}^{rt} = \kappa_{ji}^t + \varepsilon_{ji}^{rt}, \quad (3)$$

where the parameter κ_{ji}^t is the alternative-specific constant. This term includes all factors that influence the decision to purchase an EV, but that are exogenous to the optimisation model (e.g. socio-demographic characteristics). In general, the alternative-specific constants can be any function which does not depend on the decision variables.

The set C_i^{1t} includes the alternatives for charging stations which have a non-zero probability of being chosen (e.g. sufficiently close to be considered). In other words, C_i^{1t} is composed of all of the charging station alternatives that would be included in $C_i^t(\mathbf{y})$ if those stations were open. The general choice set $C_i^t(\mathbf{y})$ is thus given by

$$C_i^t(\mathbf{y}) = C_i^{0t} \cup \{j \in C_i^{1t} | y_j^t = 1\}.$$

If station $j \in C_i^{1t}$ is open, we consider the utility u_{ji}^{rt} to be a function of the number of charging outlets available at that station as well as the alternative-specific constant. This leads to the formulation

$$u_{ji}^{rt} = \sum_{k=1}^{m_j} \beta_{jik}^t x_{jk}^t + \kappa_{ji}^t + \varepsilon_{ji}^{rt}.$$

The parameter β_{jik}^t is the utility coefficient associated with having k charging outlets at station j . We note that the model does not impose any restrictions on the form of the

utility coefficients, however for logistic purposes and realism, the coefficients should be non-decreasing in k . As before, the alternative-specific constant can be any function which does not depend on the decision variables.

To ensure that the alternative associated with a closed station $j \in C_i^{1t}$ cannot be chosen, we set the simulated utility u_{ji}^{rt} to a lower bound if $y_j^t = 0$. This concept is referred to as the “discounted utility” in Pacheco Paneque et al. (2021). Let $a_{ji}^{rt} = \kappa_{ji}^t + \varepsilon_{ji}^{rt}$ and $b_{ji}^{rt} = \beta_{jim_j}^t + \kappa_{ji}^t + \varepsilon_{ji}^{rt}$ be respectively lower and upper bounds on the simulated utility u_{ji}^{rt} . Let $\bar{a}_i^t = \min \left(\left\{ a_{ji}^{rt}, j \in C_i^{1t}, 1 \leq r \leq R_i \right\} \right)$ and $\nu_{ji}^t = b_{ji}^{rt} - \bar{a}_i^t$. For each $i \in N$, we assume that R_i is sufficiently large such that for each $1 \leq t \leq T, 1 \leq r \leq R_i$ we have $\bar{a}_i^t < u_{0i}^{rt}$.

The linear formulation for the simulated utility u_{ji}^{rt} is given by

$$u_{ji}^{rt} \geq \bar{a}_i^t, \quad j \in C_i^{1t}, i \in N, 1 \leq r \leq R_i, 1 \leq t \leq T, \quad (4)$$

$$u_{ji}^{rt} \leq \bar{a}_i^t + \nu_{ji}^{rt} y_j^t, \quad j \in C_i^{1t}, i \in N, 1 \leq r \leq R_i, 1 \leq t \leq T, \quad (5)$$

$$u_{ji}^{rt} \geq \sum_{k=1}^{m_j} \beta_{jik}^t x_{jk}^t + \kappa_{ji}^t + \varepsilon_{ji}^{rt} - \nu_{ji}^{rt} (1 - y_j^t), \quad j \in C_i^{1t}, i \in N, 1 \leq r \leq R_i, 1 \leq t \leq T, \quad (6)$$

$$u_{ji}^{rt} \leq \sum_{k=1}^{m_j} \beta_{jik}^t x_{jk}^t + \kappa_{ji}^t + \varepsilon_{ji}^{rt}, \quad j \in C_i^{1t}, i \in N, 1 \leq r \leq R_i, 1 \leq t \leq T. \quad (7)$$

For each $i \in N, 1 \leq r \leq R_i, 1 \leq t \leq T$, the value of w_{ji}^{rt} for $j \in C_i^{0t} \cup C_i^{1t}$ is then given by the solution of the following optimisation problem, which acts as the lower-level problem in our bilevel optimisation model:

$$\text{Maximise } \sum_{j \in C_i^{0t}} w_{ji}^{rt} u_{ji}^{rt} + \sum_{j \in C_i^{1t}} w_{ji}^{rt} u_{ji}^{rt}, \quad (8a)$$

$$\text{subject to } \sum_{j \in C_i^{0t}} w_{ji}^{rt} + \sum_{j \in C_i^{1t}} w_{ji}^{rt} = 1, \quad (8b)$$

$$w_{ji}^{rt} \in \{0, 1\}, \quad j \in C_i^{0t} \cup C_i^{1t}. \quad (8c)$$

It is easy to see that the binary requirements can be relaxed.

4.2 Upper-Level Problem

The placement of charging outlets and stations in the upper-level is restricted by the following set of constraints

$$\sum_{j \in M} \sum_{k=1}^{m_j} kc_j^t (x_{jk}^t - x_{jk}^{t-1}) + \sum_{j \in M} f_j (y_j^t - y_j^{t-1}) \leq B^t, \quad 1 \leq t \leq T. \quad (9)$$

$$\sum_{k=1}^{m_j} x_{jk}^t = y_j^t, \quad j \in M, 1 \leq t \leq T, \quad (10)$$

$$\sum_{k=1}^{m_j} kx_{jk}^t \geq \sum_{k=1}^{m_j} kx_{jk}^{t-1}, \quad j \in M, 1 \leq t \leq T, \quad (11)$$

$$y_j^t \geq y_j^{t-1}, \quad j \in M, 1 \leq t \leq T. \quad (12)$$

Constraints (9) ensure that the amount spent opening charging stations and installing charging outlets does not exceed the budget for that period. It would also be possible to supplement the per-period budget with an overall budget, as was done in Anjos et al. (2020).

Constraints (10) force the optimisation model to install one or more charging outlets in order to open a station. The use of the equality in the constraint forces the optimisation model to install an outlet to open a station. This assumption can be relaxed however, it would thus be necessary to replace y_j^t by $\sum_{k=1}^{m_j} x_{jk}^t$ in all of the lower-level constraints.

Constraints (11) and (12) forbid the model from removing charging outlets and closing charging stations, respectively. These constraints assume that it would be suboptimal to remove a station. We note that in the first period, it is necessary to replace the right-hand sides of (11) and (12) by the initial conditions x_j^0 and y_j^0 respectively.

4.3 Bilevel Model

We now introduce the full, bilevel model

$$\text{Minimise } \sum_{t=1}^T \sum_{i \in N} N_i^t \frac{1}{R_i} \sum_{r=1}^{R_i} w_{0i}^{rt}, \quad (13)$$

subject to (3), (4) – (7), (9) – (12)

$$w_{ji}^{rt} \in \arg \max \left\{ \sum_{j \in C_i^{0t}} w_{ji}^{rt} u_{ji}^{rt} + \sum_{j \in C_i^{1t}} w_{ji}^{rt} u_{ji}^{rt} : (8b) - (8c) \right\}$$

$$x_{jk}^t, y_j^t \in \{0, 1\}.$$

We consider the *optimistic* version of the bilevel problem which means that the users do not select the opt-out alternative if a different alternative has equal utility. While this in theory

has a zero probability (given that the error terms are drawn from continuous distributions), this can occur in practice due to numerical precision.

In order to solve the model, we reformulate it as a single-level optimisation problem by transforming the lower-level model (8) into a series of constraints for the upper-level model. To this end, we apply the Karush-Kuhn-Tucker conditions which are necessary and sufficient for the optimality of the (linear) lower-level problem (Sinha et al. 2017), and we linearize the terms $w_{ji}^{rt} \cdot u_{ji}^{rt}$ through Big-M constraints. In this way, for each $i \in N, 1 \leq r \leq R, 1 \leq t \leq T$, the lower-level problem (8) is replaced by the following constraints:

$$u_{ji}^{rt} - \alpha_i^{rt} + (1 - w_{ji}^{rt}) \mu_{ji}^{rt} \geq 0, j \in C_i^{0t} \cup C_i^{1t}, \quad (14)$$

$$\sum_{j \in C_i^{0t}} w_{ji}^{rt} + \sum_{j \in C_i^{1t}} w_{ji}^{rt} = 1, \quad (15)$$

$$\alpha_i^{rt} \geq u_{ji}^{rt}, j \in C_i^{0t} \cup C_i^{1t}, \quad (16)$$

$$w_{ji}^{rt} \in \{0, 1\}, j \in C_i^{0t} \cup C_i^{1t}, \quad (17)$$

$$\alpha_i^{rt} \in \mathbb{R}, \quad (18)$$

where the Big-M constants, μ_{ji}^{rt} , are given by

$$\mu_{ji}^{rt} = \begin{cases} \max(\{b_{ji}^{rt}, j \in C_i^{1t}\} \cup \{\kappa_{ji}^{rt} + \varepsilon_{ji}^{rt}, j \in C_i^{0t}\}) - \kappa_{ji}^{rt} - \varepsilon_{ji}^{rt}, & j \in C_i^{0t}, \\ \max(\{b_{ji}^{rt}, j \in C_i^{1t}\} \cup \{\kappa_{ji}^{rt} + \varepsilon_{ji}^{rt}, j \in C_i^{0t}\}) - \bar{a}_i^t, & j \in C_i^{1t}. \end{cases}$$

We refer to the complete model with the constraints (14)-(18) as the ‘Single-Level model’ in order to distinguish from the general context of single-level reductions.

5 Maximum Covering Model

While the Single-Level model is a mixed-integer linear optimisation problem that can be given directly to a general purpose solver, large-scale instances can be hard to solve. This is due to the Big-M constraints for the utility (4)-(7) and the linearised lower-level problem (14)-(18), as well as the three sets of binary variables $\mathbf{x}, \mathbf{y}, \mathbf{w}$. In practice, the model is intractable for all but the simplest of instances. For this reason, we propose to reformulate the problem into a maximum covering problem using the pre-computed error terms ε_{ji}^{rt} .

Let $(t, i, r), 1 \leq t \leq T, i \in N, 1 \leq r \leq R_i$ be a triplet, representing scenario r of user class i in period t . For $j \in C_i^{1t}$, define

$$u_{jik}^{rt} = \beta_{jik}^t + \kappa_{ji}^t + \varepsilon_{ji}^t.$$

In other words, u_{jik}^{rt} is the utility for the triplet (t, i, r) for charging station j having k outlets in period t . This is equivalent to the utility u_{ji}^{rt} with $x_{jk}^t = 1, x_{jk'}^t = 0$ if $k' \neq k$.

Definition 5.1. A charging station j with k charging outlets covers the triplet (t, i, r) if the following conditions hold: (i) $k \geq 1$, (ii) $j \in C_i^{1t}$, and (iii) $u_{jik}^{rt} \geq u_{0i}^{rt}$, where u_{0i}^{rt} represents the opt-out utility for triplet (t, i, r) .

We say that (t, i, r) is covered by \mathbf{x} if $\exists j \in M, \exists k \in 1, \dots, m_j$ such that $x_{jk}^t = 1$ and charging station j with k charging outlets covers (t, i, r) .

Intuitively, a charging station covers a triplet if the station has at least one outlet (and is thus open), it is available to and considered by the user class in question, and the charging station is a better option than the opt-out for that triplet.

Example 5.2. We consider a given scenario r , user class i , and period t . In Figure 2, we see the utilities u_{ji}^{rt} for each option $j \in C_i^{0t} \cup C_i^{1t}$. For each option, the error terms and alternative-specific constants are all precomputed, which defines the values for utility with no charging outlets. The opt-out utility does not depend on the number of outlets, and so it is constant.

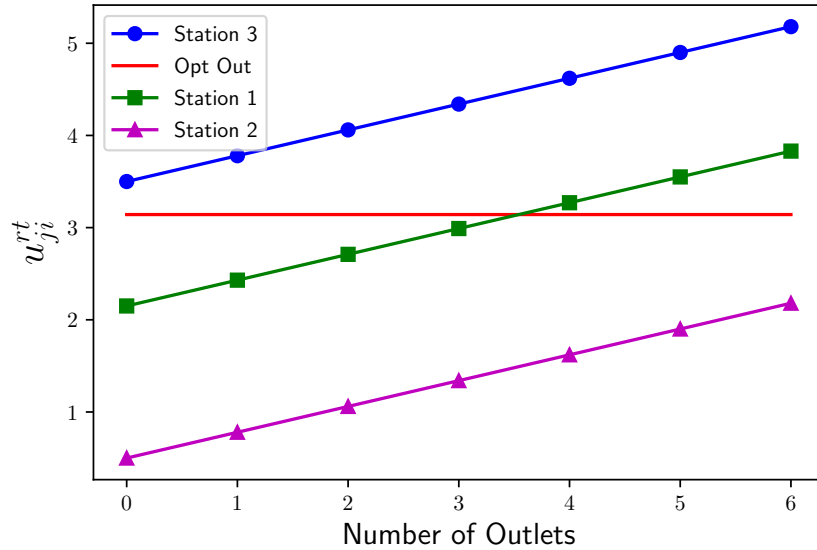


Figure 2: Utilities for user class i , under scenario r , at period t .

In this example, stations 1 and 3 only cover the triplet (t, i, r) if they have at least one and four outlets, respectively. Station 2 is not able to cover (t, i, r) even with six outlets.

Next, we define

$$a_{jik}^{rt} = \begin{cases} 1, & \text{if station } j \text{ with } k \text{ outlets covers } (t, i, r), \\ 0, & \text{else.} \end{cases}$$

This vector a of parameters can be pre-computed after the error terms have been calculated.

In the maximum covering formulation, we keep the variables (\mathbf{x}, \mathbf{y}) and we introduce the following decision variables related with the cover definition:

$$w_i^{rt} = \begin{cases} 1, & \text{if } (t, i, r) \text{ is covered by } \mathbf{x}, \\ 0, & \text{else.} \end{cases}$$

The Maximum Covering model is then

$$\text{Maximise } \sum_{t=1}^T \sum_{i \in N} \sum_{r=1}^{R_i} \frac{N_i^t}{R_i} w_i^{rt}, \quad (19)$$

subject to (9) – (12)

$$\begin{aligned} \sum_{j \in M} \sum_{k=1}^{m_j} a_{jik}^{rt} x_{jk}^t &\geq w_i^{rt}, \quad i \in N, 1 \leq r \leq R_i, 1 \leq t \leq T, \\ x_{jk}^t &\in \{0, 1\} \quad j \in M, 1 \leq k \leq m_j, 1 \leq t \leq T, \\ y_j^t &\in \{0, 1\} \quad j \in M, 1 \leq t \leq T, \\ w_i^{rt} &\in [0, 1] \quad i \in N, 1 \leq r \leq R_i, 1 \leq t \leq T. \end{aligned} \quad (20)$$

The objective function (19) is the maximisation equivalent to the objective in the bilevel model (13). Constraints (20) model whether the triplet (t, i, r) is covered by a given \mathbf{x} . We note that due to the direction of the optimisation, these inequalities are satisfied with equality at an optimum. Since these constraints are the only ones on the variables w_i^{rt} , it is well-known that their integrality can be relaxed (Murray 2016). These constraints replace the utility constraints for choice set C_i^{0t} (3), the utility constraints for choice set C_i^{1t} (4)-(7) and the lower-level problem constraints (14)-(18).

6 Heuristic Methods

While the reformulation from the bilevel model to the Maximum Covering model significantly improves tractability, the latter is still unable to solve larger instances, as shown in Section 7. We propose three heuristic methods for solving the Maximum Covering model, including rolling horizon, greedy, and Greedy Randomised Adaptive Search Procedure (GRASP).

We note that, for the greedy and GRASP methods, it is required to calculate the quality of a candidate solution \mathbf{x} . We denote

$$f(\mathbf{x}) = \sum_{t=1}^T \sum_{i \in N} \sum_{r=1}^{R_i} \frac{N_i^t}{R_i} w_i^{rt}, \quad (21)$$

with $w_i^{rt} = \min \left(1, \sum_{j \in M} \sum_{k=1}^{m_j} a_{jik}^{rt} x_{jk}^t \right)$.

6.1 Rolling Horizon Heuristic

Rolling horizon is a standard heuristic in a multi-period setting, where the model is solved independently for each period. We use this approach as a baseline. More precisely, we solve the Maximum Covering model for one period at a time, $1 \leq t \leq T$. In the first iteration, period $t = 1$, for constraints (9), (11), and (12), we set $\sum_{k=1}^{m_j} kx_{jk}^{t-1} = x_j^0, y_j^{t-1} = y_j^0$. We continue iteratively in this way until the model is solved for all periods $1 \leq t \leq T$. Given the potential difficulty of solving the Maximum Covering model even when restricted to one period, a time limit is added. The best incumbent solution found within this time limit is returned by the heuristic.

6.2 Greedy Heuristics

The maximum covering problem is generally attributed to Church and ReVelle (1974), where they also present a simple greedy heuristic. The algorithm presented here (Algorithm 1) is a natural extension, where we iteratively place one outlet at a charging station (steps 4-6), selecting the station which maximises the number of new EVs (step 3). This iteration continues for a given period until either the budget or maximum outlets per station does not permit adding any new outlets, or the total number of EVs does not increase after adding a station. The algorithm then proceeds to the next period (steps 8-10) and repeats the process.

Instead of placing one outlet at a time, it is also possible to place the maximum number of outlets when selecting the charging station. However, this version was found to perform significantly worse.

When considering the number of new EVs gained from placing an outlet, there are two possible search modes. In the *myopic* search mode, only new EVs from the current period are considered. In the *hyperoptic* search mode, all new EVs from the outlets in all future periods are considered. Both search modes are tested and compared in Section 7.

6.3 GRASP

GRASP is characterised by two phases. The first utilises a greedy approach to generate solutions, where each greedy move is randomly selected from all possible moves that result in a solution with an objective value that is within a factor α of the optimal greedy move. The second phase performs a local search procedure on each solution from the first phase. This method was first applied to the maximum covering problem by Resende (1998). However, the algorithm described in this work makes several adaptations in order to support the multi-period and sizing considerations.

6.3.1 First phase

The solution construction phase is similar to the Greedy algorithm, with the addition of the parameter $\alpha \in [0, 1]$. We randomly select one outlet to place from amongst the set of outlets

Algorithm 1 Greedy Heuristic

```
1: Initialise:  $\mathbf{x}^* \leftarrow \mathbf{x}^0$ ,  $t \leftarrow 1$ 
2: while  $t < T$  do
3:   Find the station  $j$  at which to place an outlet, which remains feasible and increases the
   objective value the most
4:   Set  $\mathbf{x}$  as  $\mathbf{x}^*$  with one additional outlet at station  $j$ 
5:   if  $f(\mathbf{x}) > f(\mathbf{x}^*)$  then
6:      $\mathbf{x}^* \leftarrow \mathbf{x}$ 
7:     Go to line 3
8:   else
9:      $t \leftarrow t + 1$ 
10:  end if
11: end while
12: return  $\mathbf{x}^*$ 
```

that result in an increase within $100 \times \alpha$ % of the best possible outlet. The myopic and hyperoptic search modes also apply in the GRASP method.

6.3.2 Solution Filtering

In our method, the second phase of GRASP takes considerably longer than the first phase. As such, it is beneficial to filter out unpromising solutions early on. In a method proposed in Resende and Ribeiro (2018), we examine whether the local search method, when applied to a candidate solution, is likely to result in a better objective value than our incumbent solution. For a given number of candidate solutions, we examine the relative increase to the objective function before and after applying the local search. For all subsequent candidate solutions, we then estimate the maximum objective value from the second phase by multiplying the objective value of the candidate solution by the maximum relative increase that was observed. If this results in an objective value that is less than our current best, we filter the candidate solution and do not start the second phase.

6.3.3 Second Phase

When examining a candidate solution $\hat{\mathbf{x}}$, we consider the three following moves:

Add: If the budget permits, we add an outlet to the given station j in period t . To ensure feasibility of the solution, we also increase the number of outlets for all subsequent periods $t + 1, \dots, T$ for station j .

Transfer: If the station j has at least one outlet, we consider each station $j', j' \neq j$, and transfer all resources spent on station j in each period $t, t + 1, \dots, T$ to be spent on station j' instead. To ensure feasibility of the solution, we set the number of outlets

at station j for periods $t' \geq t$ to the value in period $t - 1$ (or x_j^0 if $t = 1$). If station j' reaches the maximum number of outlets and there are resources remaining, they are spent on station j .

Split: If the station j has at least one outlet, we consider each station $j', j' > j$, and we evenly split the resources spent on stations j and j' in each period $t, t + 1, \dots, T$. We note that this move is symmetric, and so it is only necessary to attempt this move if $j' > j$. In order to ensure feasibility of the solution, we can only use this move if the resources spent on these stations and the prior values of the solution for these stations in period $t - 1$ allow us to open both stations and place at least one outlet in each.

The moves can be applied to the candidate solution using either the “first improvement” or “best improvement” methods as described in Resende and Ribeiro (2018). In the first improvement method, the candidate solution $\hat{\mathbf{x}}$ is updated whenever a move is found which improves the objective function $f(\hat{\mathbf{x}})$. In the best improvement method, the candidate solution $\hat{\mathbf{x}}$ is updated with the move from amongst all stations j which resulted in the highest objective function $f(\hat{\mathbf{x}})$.

6.3.4 Stopping Criteria

We wish to prevent the local search from spending considerable time making very minor improvements to the candidate solution. At the end of each loop through the stations, we check the increase in the objective function via the local search. If the relative increase to the objective function falls below a given threshold, the local search immediately ends the search in the given period and proceeds to the following one.

The GRASP algorithm terminates when one of the following conditions have been satisfied: i) a threshold number of candidate solutions have been examined, ii) a threshold number of candidate solutions have been filtered out or, iii) a time limit has been reached.

7 Computational Results

In this section, we analyse the results from computational experiments using the models and heuristic methods discussed in the previous sections. In Section 7.1, we describe the network and datasets used in our experiments. In Section 7.2, we compare the capabilities of the Growth Function model and the Maximum Covering model. The aim is to show that the Maximum Covering model can more accurately reflect effects which are known from the literature to affect EV purchase. Finally, in Section 7.3, we compare the heuristic methods presented in Section 6.

All tests were run on a server running Linux version 3.10, with an Intel Core i7-4790 CPU with eight virtual cores and 32 GB of RAM. The code was written in Python 3.7, and is available at <https://github.com/StevenLamontagne/EVChargingStationModel>. We use

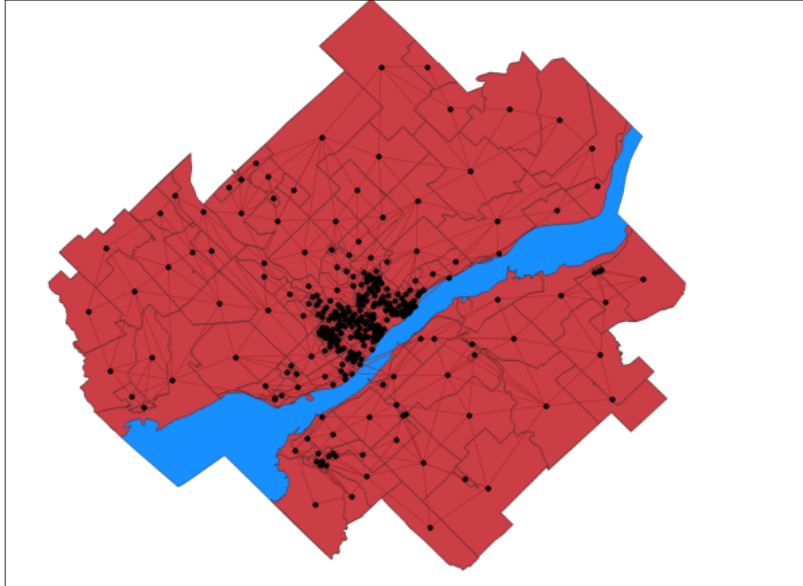


Figure 3: Trois-Rivières network

CPLEX version 12.10, accessed via the DoCPLEX module (version 2.21). Parameter values can be found in Appendix A, and instances used in the simulations are available upon request.

7.1 Test Environment

The network used for the simulations is based on the smallest aggregation level in the 2016 census (Statistics Canada 2017) for the city of Trois-Rivières, Québec. This defines 317 zones within the city, with populations and aggregate characteristics given for each zone. Nodes in the graph are given by the centroids of each zone. The edges in the graph are created between adjacent zones, with the edge length being the Euclidean distance between the centroids. We note that the Saint Lawrence river divides the city into two parts. Edges have been added to the graph to account for the Laviolette bridge, which connects both parts. The network is shown in Figure 3, with the nodes shown as points.

We generated five datasets of instances, each including a list of candidate stations, a set of user classes, and pre-computed error terms. The parameters and the generation method for the error terms for each dataset are discussed in Appendix A, with key parameter values given in Table 6. We give a summary of the important distinctions in each dataset:

Simple A small-scale dataset, which uses a simple value for each of the key parameters. This is the only dataset which the Single-Level model can solve.

Distance This dataset increases the penalisation term in the alternative-specific constant for

each station to account for distance.

HomeCharging For this dataset, we create two user classes in each node: one with and one without access to home charging.

LongSpan This dataset increases the number of years from four to ten, but the user classes remain consistent across the planning horizon.

Price In this dataset, we simulate a decrease in the price of the EV year-by-year, which affects user classes differently based on their income. The alternative-specific constant for each station is modified based on the income level of the user class and the current year.

The Simple, Distance, and HomeCharging datasets have a candidate location set with ten options, and users will not consider any station which is more than ten kilometres away. In contrast, the LongSpan and Price datasets have a candidate location with 30 options, and users may consider any charging station regardless of the distance. This results in significantly more difficult problems to solve. In general, CPLEX is not able to solve the exact model in these instances due to memory limitations.

7.2 Comparing Maximum Covering Model and Growth Function Model

We compare the capabilities of the Growth Function model with those of the Maximum Covering model. To accurately compare the models, we only use the node-based, intracity part of the Growth Function model. Parameter values are chosen to match as closely as possible between both models. The modified Growth Function model, as well as the parameters, are presented in Appendix B.

We assume that the capacity of each charging outlet is infinite in the Growth Function model. This is consistent with the assumption in the Maximum Covering model that the stations are uncapacitated.

In Sections 7.2.1 and 7.2.2, we consider two cases. In the first case, we force the solver to use the same solution for both the Growth Function and the Maximum Covering models. This allows for comparing the spread of EVs around charging stations. In the second case, we find the solution returned by the solver for the Growth Function model. We then calculate the objective value of the Maximum Covering model using that solution (by using (21)). This allows us to analyse if the differences in the spread of EVs has an impact on solution quality.

7.2.1 Distance to Charging Station

Distance is a key factor in determining which facility users choose to patronise in the maximum capture problem (Benati and Hansen 2002, Eiselt et al. 2019) as well as in models that examine existing EV owners' choice of charging location (Luo et al. 2015, Vermeulen et al. 2019, Wolbertus et al. 2021). These works all find that users are less likely to select a facility

	Growth Function	Growth Function (Adjusted)	Maximum Covering
5th percentile	9117.18	12954.33	16496.45
Median	9266.85	13113.74	16592.65
95th percentile	9407.89	13244.96	16764.57

Table 2: Number of EVs from the solutions of the Growth Function and Maximum Covering models.

as the distance increases. To our knowledge, there are no studies which examine the impact of the distance of charging stations to users in the decision to purchase an EV, but we assume that similar results hold in this case. That is, the utility of a charging option (and thus the likelihood that the charging option acts as a primary recharging method) decreases with distance.

In the Growth Function model, all users have a maximum distance within which they consider charging stations. At a given node, users consider charging at any charging station within that maximum distance.

In the Maximum Covering model, we also assume that the users have a maximum distance for considering charging stations. However, additionally, the utility decreases with distance. For this comparison, we use the Distance dataset described in Section 7.1.

In Figure 4, we see the percentage of the population that purchases an EV (at the end of the planning horizon) when one station is opened. On the left, in the Growth Function model, we see that the EV adoption rate is the same across the entire region that considers that station. By comparison, on the right in the Maximum Covering model, we see that the EV adoption rate decreases as the distance increases.

In Table 2, we report the value of (21) for the solutions from both models. We see that the optimal objective values for the Growth Function model are around 42% lower than those for the Maximum Covering model. However, the incentive for the Growth Function model to place more outlets is linked to the capacity of each station. Thus, in the uncapacitated case, it will only place one outlet at any station it opens. To counteract this effect and compare the models more fairly, we examine the objective values of adjusted solutions. These set the capacity of each station selected to be open by the Growth Function model to its maximum capacity of 6 outlets. Despite this being an infeasible solution (due to the budget), the optimal objective values for the adjusted Growth Function model are still around 20.6% lower than those for the Maximum Covering model.

We note the difference in the spread of EVs observed in Figure 4, with the spread in the Maximum Covering case being more consistent with the literature. Additionally, as we report in Table 2, the quality of the solutions are considerably different between the two models. This indicates that these differences have an important impact in the solutions, and highlights the benefits of the Maximum Covering formulation.

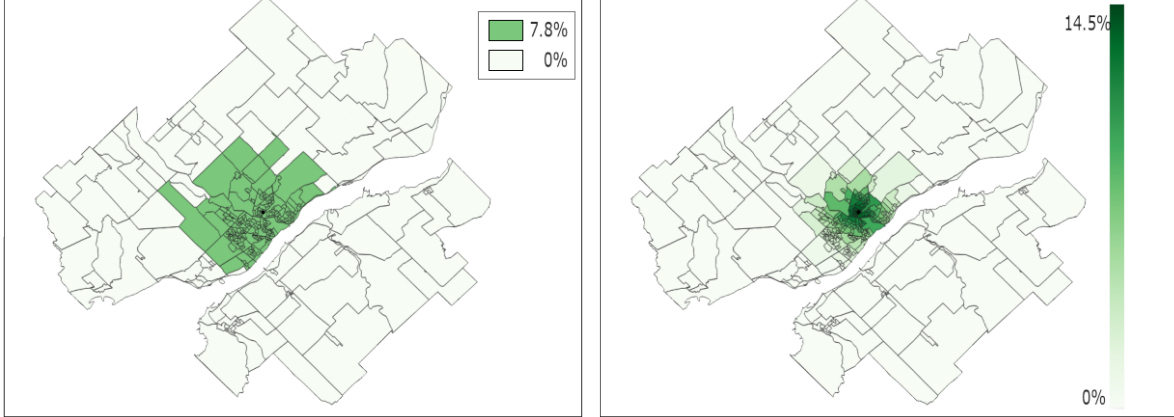


Figure 4: Percentage of population in each zone which purchases an EV by the end of the simulation when examining the distance to the charging station. Growth Function model on left side, Maximum Covering model on right side.

7.2.2 Access to Home Charging

Given it is a significant factor in the decision to purchase an EV, accurately modelling access to home charging is critical. (Hidrue et al. 2011, Bailey et al. 2015)

In the Growth Function model, it is assumed that a given fraction of new EV owners will have access to home charging (which depends on the year, but not the location). The total number of EVs at each location, including both those who have access to home charging and those who do not, is then bound by the capacity of nearby stations. Consequently, if there are no charging outlets sufficiently close to the users, not even those with home charging access may purchase EVs. We note this effect in Figure 6.

In the Maximum Covering model, the population and home charging access for each user class can be set independently. By creating two user classes for each area, with appropriately set populations, we can more accurately model the percentage of the population that has access to home charging. Additionally, since the two user classes are separate in the model, the users who have access to home charging are allowed to purchase EVs, even if no public charging infrastructure is sufficiently close. For this comparison, we use the HomeCharging dataset described in Section 7.1.

In Figure 5, we depict the percentage of the population at each area that purchase EVs by the end of the simulation period simply because of home charging access (according to the Maximum Covering model). In other words, even if no public charging infrastructure is installed, these users can charge at home and decide to purchase an EV. By contrast, in Figure 6, we depict the percentage of the population at the end of the simulation period that purchase EVs when one station is opened. On the left, in the Growth Function model, we note that only users near the charging station have purchased EVs. By comparison on the

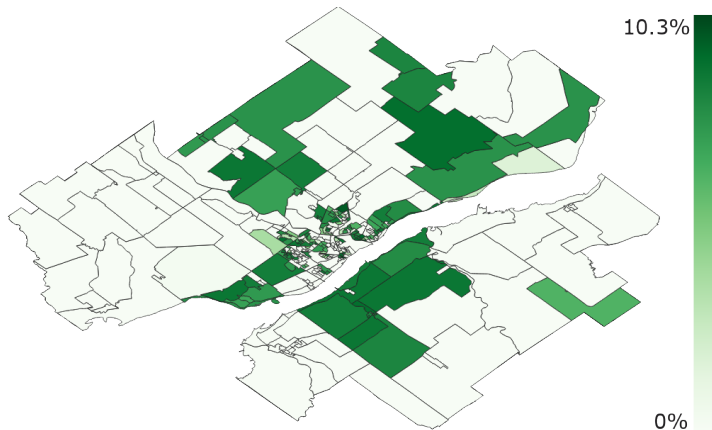


Figure 5: Percentage of Population Covered by Home Charging Access.

	Growth Function	Growth Function (Adjusted)	Maximum Covering
5th percentile	13648.43	15990.52	17975.55
Median	13737.12	16091.57	18036.37
95th percentile	13780.56	16133.63	18085.95

Table 3: Number of EVs from the solutions of the Growth Function and Maximum Covering models.

right, in the Maximum Covering model, we note that the users that were covered by home charging in Figure 5 have purchased EVs. Additionally, we see that near the charging station there is an increase to the percentage of the population that purchases EVs, as users who were not covered by home charging access are now covered by the charging station.

In Table 3, we report the value of (21) for the solutions from both models. We see that not accounting for home charging access results in a decrease in the number of EVs of around 23.8%. As before, we examine an adjusted solution to take the infinite capacity into account. Despite this being an infeasible solution, it results in a decrease in the numbers of EVs of around 10.8% compared to the Maximum Covering model.

Clearly, the same findings emerge as in Section 7.2.1.

7.3 Comparing Heuristics

We compare the Maximum Covering model from Section 5 (labelled as “Exact” in the results) and the heuristics presented in Section 6, with a time limit of two hours (7,200 seconds) imposed for all methods. The Greedy procedure is tested using both the myopic and hyperoptic search methods. For the Rolling Horizon method, we examine two ways of distributing the time across the years. In the first, we divide the time evenly amongst all years (“Even”).

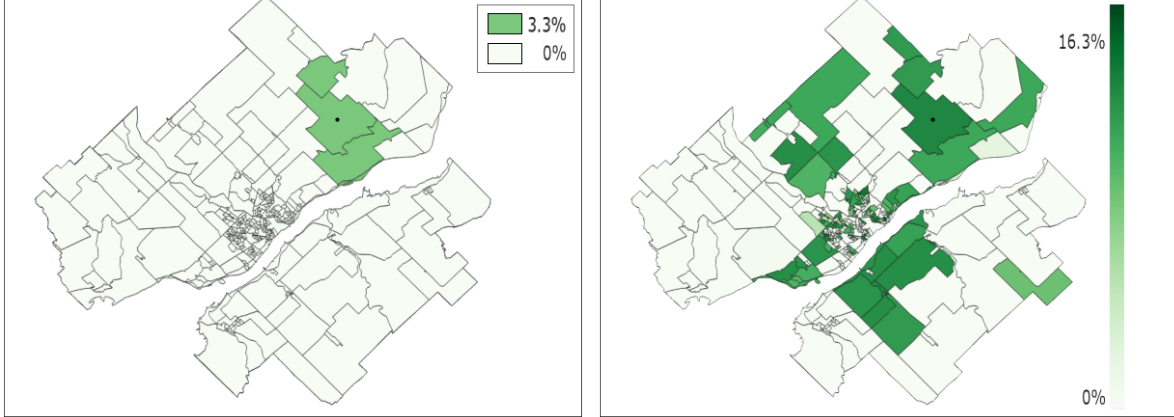


Figure 6: Percentage of population in each zone which purchases an EV by the end of the simulation when examining the home charging access. Growth Function model on left side, Maximum Covering model on right side.

In the second, the time limit is divided geometrically, with the first year having a time limit of 3,600 seconds and each successive year having half of the previous time (“Geometric”). For the GRASP procedure, we test both the myopic and hyperoptic search methods. We set the value of α to 0.85, as recommended for the maximum covering problem in Resende and Ribeiro (2018). The GRASP procedures run until 300 solutions have been examined, or until 500 solutions have been filtered out. The second phase of the GRASP procedure uses the first improvement method.

7.3.1 Solving Time

In Table 4, we report the 5th percentile, 95th percentile, and the median of the solving times for all instances of a given dataset and method.

The Exact method was able to solve the small datasets (Simple, Distance, HomeCharging) quickly, beaten only by the Greedy methods. However, the solving times for the LongSpan and Price datasets generally reach the time limit. We also note the 5th percentile for solving of the Exact method in the Price dataset is 240.58 seconds; due to the high number of variables and constraints, the solver often ran out of memory well before the time limit was reached. Both Greedy methods are undoubtedly the fastest, taking at least an order of magnitude less time than any other heuristic method, even in the small datasets.

The Rolling Horizon methods both solve relatively quickly for the small datasets. In the LongSpan test set, the Rolling Horizon methods solve more quickly than the Exact method. Since the user classes are the same for each year, solutions from previous years act as good quality warmstart solutions. This allows the later years in the Rolling Horizon method to solve before the time limit. However, the opposite occurs in the Price test set, with the Rolling

		Simple	Distance	HomeCharging	LongSpan	Price
Exact	5th percentile	0.32	0.92	3.64	7204.86	240.58
	Median	0.37	1.18	7.87	7206.64	7200.00
	95th percentile	0.41	1.43	15.88	7208.13	7207.00
Greedy (Myopic)	5th percentile	0.10	0.15	0.15	1.17	1.03
	Median	0.10	0.16	0.29	1.18	1.05
	95th percentile	0.10	0.17	1.07	1.65	1.09
Greedy (Hyperoptic)	5th percentile	0.21	0.29	0.29	4.98	2.20
	Median	0.21	0.30	0.43	5.00	2.25
	95th percentile	0.21	0.33	1.19	5.12	2.36
RollingHorizon (Even)	5th percentile	8.23	14.67	29.58	2802.14	8484.12
	Median	8.29	15.00	48.72	3048.52	8511.06
	95th percentile	8.36	15.17	100.36	3140.20	9028.46
RollingHorizon (Geometric)	5th percentile	8.33	14.98	29.51	6658.29	8511.97
	Median	8.39	15.07	49.08	6780.89	8516.48
	95th percentile	8.57	15.17	68.36	7002.04	8524.45
GRASP (Myopic)	5th percentile	66.48	78.20	88.06	1593.75	851.76
	Median	70.24	83.71	90.22	1643.60	873.17
	95th percentile	81.70	87.18	101.45	1666.46	896.95
GRASP (Hyperoptic)	5th percentile	99.27	119.29	128.16	3058.92	1405.71
	Median	104.55	122.83	131.36	3117.69	1430.74
	95th percentile	113.94	127.47	138.17	3197.92	1478.21

Table 4: Comparison of solving times for heuristic methods in a variety of test settings. Times are given in seconds.

Horizon methods taking longer to solve than the exact method. Since the user classes change each year, the quality of the solution for previous years is poorer, which causes the solver to reach the time limit. The additional overhead between each iteration, as well as CPLEX slightly exceeding the time limit in each iteration, then causes the Rolling Horizon methods to take longer than the Exact method.

While the GRASP methods took longer to solve than the RollingHorizon methods in the small datasets, they scaled much better for the Price dataset. This resulted in a solving time around a sixth that of the RollingHorizon and Exact methods. In the LongSpan dataset, the solving times for the GRASP method are quite high. This is due to the fact that both the first and second phases iterate over every year, which causes the solving time to increase substantially as the number of time years increases. The hyperoptic method solved noticeably slower than the myopic method.

7.3.2 Solution Values

In Table 5, we report the 5th percentile, 95th percentile, and the median of the gaps to the best known solution for all instances of a given test set and method. Additionally, we give the number of instances in which a method has found a solution with objective value equal

to that of the best known solution. In the case of the Simple, Distance, and HomeCharging datasets, the exact solution is known, thus the corresponding entries for the heuristic methods are the optimality gaps.

While the Exact method produces the best solution value for the smaller tests (Simple, Distance, HomeCharging), it is unable to find good solutions in the time limit for the other datasets. On the LongSpan test set, the 5th percentile for the gap to the best solution is over 50%. In the case of the Price test set, the only solution that the solver has found is the (trivial) zero solution.

The Greedy methods performed slightly worse than the other heuristic methods in the Simple, Distance, and Home Charging datasets, but they performed surprisingly well in the LongSpan and Price datasets. They frequently found the best solution, and with gaps under 0.1% even in cases where the method did not find the best solution.

The Rolling Horizon methods perform well in the smaller test sets but, similar to the Exact method, they suffer from a longer solving time on the LongSpan and Price datasets. Both GRASP methods performed comparable to each other, and comparable with the Greedy methods.

8 Conclusion

In this work, we proposed a model for determining the optimal location of EV charging stations in a long-term planning environment so as to maximise the total number of EVs. To consider user-specific characteristics, we used discrete choice models to represent the decision of the users to purchase EVs. When compared to the existing model for this problem (the Growth Function model in Anjos et al. (2020)) this allowed for more intuitive user behaviour with regards to charging station location and home charging access. Additionally, solutions for the Growth Function model were significantly different than those for the Maximum Covering model, highlighting the benefits of using the latter.

Using the simulation-based approach of Pacheco Paneque et al. (2021) resulted in a bilevel model. By reformulating the model as a maximum covering problem, the sets of Big-M constraints were removed, thus improving the tractability. We note that this reformulation can be applied to other applications of the simulation-based method (including the MCPRU) if no capacity constraints are present.

For more difficult instances, several heuristic methods were proposed for obtaining feasible solutions. While the Rolling Horizon heuristic was not as effective for more difficult instances, the Greedy and GRASP algorithms both performed very well. In particular, we note that the Greedy methods were able to find solutions within a few seconds, even on the most difficult instances. The similar performances of the Greedy and GRASP methods suggests that more complex local search moves may be necessary to find better solutions.

While the heuristic methods were able to quickly find feasible solutions, we are not able to verify the quality of these solutions on the larger instances. Further research will examine

		Simple	Distance	HomeCharging	LongSpan	Price
Exact	5th percentile	0.00	0.00	0.00	61.14	zero
	Median	0.00	0.00	0.00	80.24	zero
	95th percentile	0.00	0.00	0.00	80.27	zero
	# of best	20	20	20	0	0
Greedy (Myopic)	5th percentile	0.00	1.66	0.46	0.00	0.00
	Median	0.00	1.94	0.50	0.00	0.01
	95th percentile	0.07	2.76	0.68	0.03	0.05
	# of best	11	0	0	12	9
Greedy (Hyperoptic)	5th percentile	0.00	1.47	0.44	0.00	0.00
	Median	0.06	1.99	0.59	0.01	0.02
	95th percentile	0.19	2.53	0.84	0.05	0.06
	# of best	9	0	0	8	5
RollingHorizon (Even)	5th percentile	0.00	0.00	0.00	2.62	11.38
	Median	0.00	0.00	0.03	4.15	11.48
	95th percentile	0.00	0.38	0.09	4.32	12.70
	# of best	20	12	7	0	0
RollingHorizon (Geometric)	5th percentile	0.00	0.00	0.00	2.41	11.50
	Median	0.00	0.00	0.03	2.50	12.35
	95th percentile	0.00	0.38	0.09	4.19	12.83
	# of best	20	12	7	0	0
GRASP (Myopic)	5th percentile	0.00	0.14	0.16	0.10	0.00
	Median	0.00	0.43	0.26	0.20	0.02
	95th percentile	0.12	0.68	0.36	0.24	0.04
	# of best	16	0	0	0	5
GRASP (Hyperoptic)	5th percentile	0.00	0.19	0.12	0.10	0.00
	Median	0.00	0.41	0.23	0.18	0.04
	95th percentile	0.16	0.67	0.36	0.26	0.07
	# of best	14	0	0	0	2

Table 5: Comparison of gaps to the best known solution for heuristic methods in all five datasets (in percentage). The 'zero' entry indicates that only the trivial zero solution was found.

an exact method specifically tailored for larger scale instances. A possible approach is the Bender’s decomposition method proposed in Cordeau et al. (2019), which is designed for large-scale maximum covering problems.

Additionally, since the Maximum Covering model was designed for the intracity network, it is not applicable to larger geographical areas. For example, in the Maximum Covering model, there are no constraints related to the range of EVs, which would be necessary for intercity travel. This is a notable difference with the Growth Function model of Anjos et al. (2020), which was designed for intracity and intercity networks, and was applied to the province of Québec. As such, further research will examine an extension of the Maximum Covering model which includes the intercity network.

Acknowledgements

The authors gratefully acknowledge the assistance of Jean-Luc Dupré from *Direction Mobilité* of *Hydro-Québec*, for both providing and helping to understand EV charging data, as well as for sharing his expertise on EV charging stations and the network. We gratefully acknowledge the work of Mahsa Moghaddass in estimating the parameter values used in the models.

This research was supported by Hydro-Québec, NSERC Collaborative Research and Development Grant CRDPJ 536757 - 19, and NSERC Discovery grant 2017-06054.

References

- Robert Aboolian, Oded Berman, and Dmitry Krass. Competitive facility location model with concave demand. *European Journal of Operational Research*, 181(2):598–619, 2007.
- Martin Achtnicht, Georg Bühler, and Claudia Hermeling. The impact of fuel availability on demand for alternative-fuel vehicles. *Transportation Research Part D: Transport and Environment*, 17(3): 262–269, May 2012.
- Miguel F. Anjos, Bernard Gendron, and Martim Joyce-Moniz. Increasing electric vehicle adoption through the optimal deployment of fast-charging stations for local and long-distance travel. *European Journal of Operational Research*, 285(1):263–278, 2020.
- Association des Véhicules Électrique du Québec. Statistiques SAAQ-AVÉQ sur l’électromobilité au Québec en date du 30 juin 2021, 2021.
- J. Axsen, S. Goldberg, J. Bailey, G. Kamiya, B. Langman, J. Cairns, M. Wolinetz, and A. Miele. Electrifying vehicles: Insights from the canadian plug-in electric vehicle study. Technical report, Simon Fraser University, 2015a.
- Jonn Axsen, Joseph Bailey, and Marisol Andrea Castro. Preference and lifestyle heterogeneity among potential plug-in electric vehicle buyers. *Energy Economics*, 50:190–201, July 2015b.
- Badak Badri-Koohi, Reza Tavakkadi-Moghaddam, and Mahnaz Asghari. Optimizing number and locations of alternative fuel stations using a multi-criteria approach. *Engineering, Technology & Applied Science Research*, 9(1):3715–3720, 2019.

- Joseph Bailey, Amy Miele, and Jonn Axsen. Is awareness of public charging associated with consumer interest in plug-in electric vehicles? *Transportation Research Part D: Transport and Environment*, 36:1–9, 2015.
- Stefano Benati. The maximum capture problem with heterogeneous customers. *Computers & Operations Research*, 26(14):1351–1367, 1999.
- Stefano Benati and Pierre Hansen. The maximum capture problem with random utilities: Problem formulation and algorithms. *European Journal of Operational Research*, 143(3):518–530, 2002.
- Oded Berman, Tammy Drezner, Zvi Drezner, and Dmitry Krass. Modeling competitive facility location problems: New approaches and results. *INFORMS TutORials in Operations Research*, 14(2014): 156–181, October 2014.
- Michel Bierlaire. Electrifying vehicles: Insights from the canadian plug-in electric vehicle study. Technical Report TRANSP-OR 200605, Transport and Mobility Laboratory, ENAC, EPFL, 2020.
- Ismail Capar et al. An arc cover–path-cover formulation and strategic analysis of alternative-fuel station locations. *European Journal of Operational Research*, 227(1):142–151, 2013.
- Richard Church and Charles ReVelle. The maximal covering location problem. *Papers of the regional science association*, 32(1):101–118, 1974.
- Makena Coffman, Paul Bernstein, and Sherilyn Wee. Electric vehicles revisited: a review of factors that affect adoption. *Transport Reviews*, 37(1):79–93, 2017.
- Jean-François Cordeau, Fabio Furini, and Ivana Ljubić. Benders decomposition for very large scale partial set covering and maximal covering location problems. *European Journal of Operational Research*, 275(3):882–896, 2019.
- Qiushi Cui, Yang Weng, and Chin-Woo Tan. Electric vehicle charging station placement method for urban areas. *IEEE Transactions on Smart Grid*, 10(6):6552–6565, November 2019.
- Tien Thanh Dam, Thuy Anh Ta, and Tien Mai. Submodularity and local search approaches for maximum capture problems under generalized extreme value models. *European Journal of Operational Research*, 2021.
- H. A. Eiselt, Vladimir Marianov, and Tammy Drezner. Competitive location models. In G. Laporte, S. Nickel, and F. Saldanha da Gama, editors, *Location Science*, chapter 14, pages 391–429. Springer, 2019.
- Environment and Climate Change Canada. Greenhouse gas sources and sinks: executive summary 2021, 2021.
- Inês Frade et al. Optimal location of charging stations for electric vehicles in a neighborhood in Lisbon, Portugal. *Transportation Research Record Journal of the Transportation Research Board*, 2252: 91–98, 2011.
- Alexandre S. Freire, Eduardo Moreno, and Wilfredo F. Yushimitoa. A branch-and-bound algorithm for the maximum capture problem with random utilities. *European Journal of Operational Research*, 252(1):204–212, 2016.
- Sebastián González, Felipe Feijooa, Franco Bassoa, Vignesh Subramanianb, Sriram Sankaranarayanananc, and Tapas Dasd. Routing and charging facility location for evs under nodal pricing of electricity: A bilevel model solved using special ordered set. *IEEE Transactions on Smart Grid*, 2022.
- Knut Haase. Discrete location planning. Technical report, Institute for Transport and Logistics Studies, University of Sydney, 2009.

- André Hackbarth and Reinhard Madlener. Consumer preferences for alternative fuel vehicles: A discrete choice analysis. *Transportation Research Part D: Transport and Environment*, 25:5–17, December 2013.
- Michael K. Hidrue et al. Willingness to pay for electric vehicles and their attributes. *Resource and Energy Economics*, 2011.
- International Energy Agency. Greenhouse gas emissions from energy: Overview, 2021.
- Roxana J. Javid and Ali Nejat. A comprehensive model of regional electric vehicle adoption and penetration. *Transport Policy*, 54:30–42, 2017.
- Ahmed Abdelmoumene Kadri, Romain Perrouault, Mouna Kchaou Boujelben, and Céline Gicquel. A multi-stage stochastic integer programming approach for locating electric vehicle charging stations. *Computers & Operations Research*, 117:104888, 2020.
- Seow Lim and Michael Kuby. Heuristic algorithms for siting alternative-fuel stations using the Flow-Refueling Location Model. *European Journal of Operational Research*, 204(1):51–61, 2010.
- Ivana Ljubić and Eduardo Moreno. Outer approximation and submodular cuts for maximum capture facility location problems with random utilities. *European Journal of Operational Research*, 266(1):46–56, 2018.
- Chao Luo, Yih-Fang Huang, and Vijay Gupta. Placement of ev charging stations—balancing benefits among multiple entities. *IEEE Transactions on Smart Grid*, 10(1109):1–10, 2015.
- Tien Mai and Andrea Lodi. A multicut outer-approximation approach for competitive facility location under random utilities. *European Journal of Operational Research*, 284(3):874–881, 2020.
- Alan T. Murray. Maximal coverage location problem: Impacts, significance, and evolution. *International Regional Science Review*, 39(1):5–27, 2016.
- Michael Nicholas, Dale Hall, and Nic Lutsey. Quantifying the electric vehicle charging infrastructure gap across U.S. markets. Technical report, International Council on Clean Transportation, 2019.
- Meritxell Pacheco Paneque et al. Integrating advanced discrete choice models in mixed integer linear optimization. *Transportation Research Part B: Methodological*, 146:26–49, 2021.
- Mauricio G.C. Resende. Computing approximate solutions of the maximum covering problem with GRASP. *Journal of Heuristics*, 4(2):161–177, 1998.
- Mauricio G.C. Resende and Celso C. Ribeiro. *Optimisation By GRASP: Greedy Randomized Adaptive Search Procedures*. Springer, 2018.
- Zeinab Rezvani, Johan Jansson, and Jan Bodin. Advances in consumer electric vehicle adoption research: A review and research agenda. *Transportation Research Part D: Transport and Environment*, 34:122–136, 2015.
- Aviral Shukla, Joseph Pekny, and Venkat Venkatasubramanian. An optimization framework for cost effective design of refueling station infrastructure for alternative fuel vehicles. *Computers & Chemical Engineering*, 35(8):1431–1438, 2011.
- Ankur Sinha, Pekka Malo, and Kalyan Deb. A review on bilevel optimization: From classical to evolutionary approaches and applications. *IEEE Transactions on Evolutionary Computation*, 22(2):276–295, 2017.
- Statistics Canada. 2016 census, catalogue no. 98-401-x2016044, 2017.
- Kenneth Train. *Discrete Choice Methods with Simulation*. Cambridge University Press, 2002.

- Igna Vermeulen, Jurjen Rienk Helmus, Mike Lees, and Robert van den Hoed. Simulation of future electric vehicle charging behavior—effects of transition from PHEV to FEV. *World Electric Vehicle Journal*, 10(2), 2019.
- Joan Walker, Moshe Ben-Akiva, and Denis Bolduc. Identification of the logit kernel (or mixed logit) model. In *10th International Conference on Travel Behavior Research*, 2004.
- Rick Wolbertus, Robert van den Hoed, Maarten Kroesen, and Caspar Chorus. Charging infrastructure roll-out strategies for large scale introduction of electric vehicles in urban areas: An agent-based simulation study. *Transportation Research Part A: Policy and Practice*, 148:262–285, 2021.
- JongRoul Woo, Hyunhong Choi, and Joongha Ahn. Well-to-wheel analysis of greenhouse gas emissions for electric vehicles based on electricity generation mix: A global perspective. *Transportation Research Part D: Transport and Environment*, 51:340–350, 2017.
- Anpeng Zhang, Jee Eun Kang, and Changhyun Kwon. Incorporating demand dynamics in multi-period capacitated fast-charging location planning for electric vehicles. *Transportation Research Part B: Methodological*, 103:5–29, 2017.
- Andreas Ziegler. Individual characteristics and stated preferences for alternative energy sources and propulsion technologies in vehicles: A discrete choice analysis for Germany. *Transportation Research Part A: Policy and Practice*, 46(8):1372–1385, October 2012.

A Parameter Values

In this section, we describe the parameter values for each dataset, as well as the mechanism for drawing error terms in each. We start by describing the general framework used for the error terms, as that is common to all of the datasets. Table 6 provides a list of parameter values, with more detailed explanations in the following subsections for parameter values which differ. Unless otherwise specified, parameter values are set arbitrarily.

In all of our datasets:

- Each user class $i \in N$ includes the home location (as a node in the network). This allows us to estimate population based on the census data (Statistics Canada 2017), with the number of user classes per node and the partitioning method depending on the dataset.
- For each $i \in N, 1 \leq t \leq T$, the alternative-specific constant for the opt-out option $\kappa_{0_i}^t$ is set to 4.5.

In order to simulate the error terms for the demand model, we employ the error components formulation of the mixed logit model to approximate a nested logit model, as described in Train (2002) and Walker et al. (2004). The notation in what follows matches the latter work, and we refer to the aforementioned work for detailed explanations of the process.

For each $i \in N, 1 \leq t \leq T, 1 \leq r \leq R_i$, the vector of error terms $\varepsilon_i^{rt} = (\varepsilon_i^{rt})_{j \in C_i^{0t} \cup C_i^{1t}}$ is given by

$$\varepsilon_i^{rt} = FT\xi^r + \zeta^r, \quad (22)$$

with

- F a *factor loading* matrix.
- T a diagonal matrix with the standard deviation of each factor.
- ξ^r a vector of IID random terms from a normal distribution.
- ζ^r a vector of IID random terms from a Gumbel distribution.

The form of the matrices F and T vary in each dataset. However, in all datasets, ξ^r has a location of zero and a scale of one, and ζ^r has location of zero and a scale of three.

A.1 Simple Dataset

The set of user classes N includes one user class for every node in the network. The population of user class i , N_i^t , is given by the population of the node in the 2016 census multiplied by a factor of 0.1. In other words, 10% of the population in each node are deciding to purchase a vehicle each year.

Parameter	Simple	Distance	HomeCharging	LongSpan	Price
T	4	4	4	10	4
$ M $	10	10	10	30	30
$ N $	317	317	734	317	1397
$ C_0^{it} $	1	2	1	1	1
$ C_1^{it} $	Varies	Varies	Varies	30	30
x_j^0 (all stations)	0	0	0	0	0
y_j^0 (all stations)	0	0	0	0	0
R_i	$15 \times C_0^{it} \cup C_1^{it} $	$15 \times C_0^{it} \cup C_1^{it} $	$15 \times C_0^{it} \cup C_1^{it} $	465	465
B^t (per year)	400	400	400	400	400
m_j (all stations)	2	6	6	6	6
f_j (all stations)	100	100	100	100	100
c_j^t (all stations and years)	50	50	50	50	50

Table 6: Maximum Covering parameter values

For each $i \in N, 1 \leq t \leq T$, the choice set C_i^{1t} includes all stations which are within ten kilometres of the location of the user class. The utility for $j \in C_i^{1t}$ is linear in terms of the number of charging outlets, with

$$\beta_{jik}^t = 0.281k, \forall j \in C_i^{1t}. \quad (23)$$

Additionally, the alternative-specific constant for each station $j \in C_i^{1t}$ is calculated as

$$\kappa_{ji}^t = 1.464\delta_1 - 0.063\delta_2 + 0.174\delta_3, \quad (24)$$

with

- δ_1 : binary coefficient indicating if the station is level 3 (i.e. fast charging). We note that in our tests all stations were considered level 3.
- δ_2 : the distance (in kilometres, shortest path in the network) between the user's home and the charging station,
- δ_3 : binary coefficient indicating if the station is in the city center (defined as a subset of the nodes in the network).

The coefficients for these parameters were estimated using real-world data. A discrete choice model was created which examined which charging station was selected by EV owners when recharging their vehicle. A multinomial logit model was estimated with the maximum likelihood approach with the BIOGEME package in Python (Bierlaire 2020), using real charging data for EV owners in the province of Québec.

For the error terms for each $i \in N, 1 \leq t \leq T$, the options $j \in C_i^{0t} \cup C_i^{1t}$ are divided into two nests: one for the opt-out option and one for all charging stations. The $|C_i^{0t} \cup C_i^{1t}| \times 2$

factor loading matrix F and 2×2 diagonal matrix T are given by

$$F = \begin{bmatrix} 1 & 0 \\ 0 & 1 \\ \vdots & \vdots \\ 0 & 1 \end{bmatrix}, \quad T = \begin{bmatrix} 1 & 0 \\ 0 & 1 \end{bmatrix}. \quad (25)$$

A.2 Distance Dataset

The user classes, choice sets, and error terms are all identical to the Simple dataset.

The coefficient for distance in the alternative-specific constant has been increased by a factor of ten. More specifically, for each $i \in N, 1 \leq t \leq T$, the alternative-specific constant for each station $j \in C_i^{1t}$ is calculated as

$$\kappa_{ji}^t = 1.464\delta_1 - 0.63\delta_2 + 0.174\delta_3, \quad (26)$$

with $\delta_1, \delta_2, \delta_3$ defined as in the Simple dataset.

A.3 Home Charging Dataset

The set of user classes N includes two user classes for every node in the network: one which has access to home charging, and one which does not. We estimate the access to home charging via the housing information in the 2016 census (Statistics Canada 2017). Based on recommendations from our industrial partners, we assume that 90% of users in single homes have access to home charging, while 75% of those in attached homes, and 40% of those in apartments also have access. The population of each of the two user classes are given by the respective estimates multiplied by a factor of 0.1.

For user classes i which have access to home charging and for each $1 \leq t \leq T$, the utility for $j \in C_i^{1t}$ is linear in terms of the number of charging outlets, with

$$\beta_{jik}^t = 0.211k, \forall j \in C_i^{1t}. \quad (27)$$

For user classes i which do not have access to home charging and for each $1 \leq t \leq T$, the utility for $j \in C_i^{1t}$ is linear in terms of the number of charging outlets, with

$$\beta_{jik}^t = 0.351k, \forall j \in C_i^{1t}. \quad (28)$$

In both cases, the choice set C_i^{1t} includes all stations which are within ten kilometres of the location of the user class and the alternative-specific constants are identical to the Simple dataset.

For user classes i which do not have access to home charging, the error terms are identical to the Simple dataset. For user classes i which have access to home charging and for each $1 \leq t \leq T$, the options $j \in C_i^{0t} \cup C_i^{1t}$ are divided into three nests: one for the opt-out option,

one for home charging, and one for all charging stations. The $|C_i^{0t} \cup C_i^{1t}| \times 3$ factor loading matrix F and 3×3 diagonal matrix T are given by

$$F = \begin{bmatrix} 1 & 0 & 0 \\ 0 & 1 & 0 \\ 0 & 0 & 1 \\ \vdots & \vdots & \vdots \\ 0 & 0 & 1 \end{bmatrix}, \quad T = \begin{bmatrix} 1 & 0 & 0 \\ 0 & 1 & 0 \\ 0 & 0 & 1 \end{bmatrix}. \quad (29)$$

A.4 LongSpan Dataset

The mechanisms for the user classes, alternative-specific constants, and error terms are all identical to the Simple dataset. However, the choice sets for each user class now include all stations, not only those within ten kilometres. This, combined with the increased number of stations and the longer time span, results in a significantly more difficult problem to solve.

A.5 Price Dataset

The alternative-specific constants, error terms, and choice sets are identical to the LongSpan dataset.

In this dataset, we simulate a price decrease year-by-year, which affects different user classes differently based on their income. The set of user classes N includes five user classes for every node in the network, based on the partitioning in Javid and Nejat (2017) for income. In the aforementioned work, a logit model for EV acquisition was estimated, with one of the considered factors being the annual household income. The income level was classified as a categorical variable, with the categories defined via income

- Less than 25 000\$,
- 25 000\$ - 49 999\$,
- 50 000\$ - 74 999\$,
- 75 000 - 99 999\$,
- Greater or equal to 100 000\$.

In the final estimation of the logit model, the income variable was found to be significantly significant. The utility coefficient for the categorical variable was estimated as 0.443.

In our work, we estimate the population in each node that falls within each of the five income brackets using the household income field in the 2016 Statistics Canada census (Statistics Canada 2017), and assigned each to a user class.¹ The population of each of the five user

¹The census provides data in brackets of 10 000\$, and so the population in certain fields was divided evenly into two user classes (e.g. half of the population of the “20 000\$ to 29 999\$” field in the census was assigned to the “Less than 25 000\$” user class whereas the other half was added to the “25 000\$ - 49 999\$” user class.)

Income level of user class i	δ_{4i}
Less than 25 000\$	-2
25 000\$ - 49 999\$	-1
50 000\$ - 74 999\$	0
75 000 - 99 999\$	1
Greater or equal to 100 000\$	2

Table 7: Values of parameter δ_{4i}

classes are given by the respective estimates multiplied by a factor of 0.1, and any user class which would have a population < 1 are removed.

An additional term is added to the alternative specific constants for all charging stations based on the income bracket, in increments of 0.443. We then modify the value of the penalisation term each year to account for a decrease in price affecting each user class differently (with the modification affecting the lower income brackets more). More specifically, for each $i \in N, 1 \leq t \leq T$, the alternative-specific constant for each station $j \in C_i^{1t}$ is calculated as

$$\kappa_{ji}^t = 1.464\delta_1 - 0.063\delta_2 + 0.174\delta_3 + 0.443\delta_{4i} + 0.443(t-1)\left(\frac{2-\delta_{4i}}{4}\right), \quad (30)$$

with $\delta_1, \delta_2, \delta_3$ defined as in the Simple dataset and δ_{4i} given in Table 7.

B Growth Function model

B.1 Intracity model

For comparing the Growth Function model of Anjos et al. (2020) to the Maximum Covering model, it must be reduced to an intracity form. More precise definitions and development of each of these variables and equations, we refer to the previous work. Note that some variable names have been changed from the original work to avoid confusion with notation in Maximum Covering and Single-Level model. We assume that the city occupies a single urban centre u . We also eliminate the path-based constraints from the optimisation model, as these represent users travelling between urban centres. Given these simplifications, we use the following notation:

- T : Set of investment periods.
- N : Set of population centers.
- M : Set of candidate locations.
- $N_j, j \in M$: Set of locations which are willing to charge at location j .

- $e_j, j \in M$: Maximum number of charging outlets at location j .
- r : Population of the city.
- r_i : Population in location i .
- $l_j, j \in M$: Number of charging outlets already installed at location j .
- c^U : Cost for installing a charging outlet at any location.
- $c_j^F, j \in M$: One-time cost for opening location j .
- $B^t, t \in T$: Budget for year t .
- α : Fraction of EV users that choose to charge at home.
- $a^t, t \in T$: Capacity increase for each charging outlet in year t .
- S : Set of segments in the (piecewise linear) growth function.
- $q^{s-1}, q^s, s \in S$: Breakpoints of segment s in the growth function.
- $m^s, s \in S$: Slope of segment s in the growth function.
- $o^s, s \in S$: Intercept of segment s in the growth function.
- $x_j^t, j \in M, t \in T$: Number of charging outlets at station i in year t .
- $y_j^t, j \in M, t \in T$: 1 if station is open in year t , 0 otherwise.
- $w^{st}, s \in S, t \in T$: 1 if the city is at penetration level s at the beginning of year t , 0 otherwise.
- $h_{ij}^t, i \in N, j \in M, t \in T$: Number of EVs based in location i choosing to charge in location j in year t .
- $z^{st}, s \in S, t \in T$: Number of EVs in the city which is at penetration level s at the beginning of year t .

The list of parameter values can be found in Table 8.

The model used for the comparisons is the following:

$$\text{Maximise } \sum_{j \in M} \sum_{i \in N_j} h_{ij}^{t-1}, \quad (31)$$

$$\text{subject to } \sum_{j \in M} c_U (x_j^t - x_j^{t-1}) + \sum_{j \in M} c_j^F (y_j^t - y_j^{t-1}) \leq B^t, \quad t \in T, \quad (32)$$

$$x_j^t \leq e_j y_j^t, \quad j \in M, 1 \leq t \leq T, \quad (33)$$

$$x_j^t \geq x_j^{t-1}, \quad j \in M, 1 \leq t \leq T, \quad (34)$$

$$y_j^t \geq y_j^{t-1}, \quad j \in M, 1 \leq t \leq T, \quad (35)$$

$$\sum_{s \in S} z^{st} = \sum_{j \in M} \sum_{i \in N_j} h_{ij}^{t-1}, \quad t \in T, \quad (36)$$

$$q^{s-1} w^{st} \leq z^{st} \leq q^s w^{st}, \quad s \in S, t \in T, \quad (37)$$

$$\sum_{s \in S} w^{st} \leq 1, \quad t \in T, \quad (38)$$

$$\sum_{i \in N_j} h_{ij}^t \leq \sum_{i \in N_j} h_{ij}^{t-1} + \frac{r_i}{r} \sum_{s \in S} (o^s w^{st} + (m^s - 1) z^{st}), \quad j \in M, t \in T, \quad (39)$$

$$\sum_{i \in N_j} h_{ij}^{t-1} \leq \sum_{i \in N_j} h_{ij}^t, \quad j \in M, t \in T, \quad (40)$$

$$\alpha \sum_{i \in N_j} h_{ij}^t \leq a^t \left(x_j^0 + \sum_{t' \leq t} x_j^{t'} \right) \quad j \in N, t \in T. \quad (41)$$

The objective function (31) aims to maximise the total number of EV users in the final year. Constraints (32) are budget constraints, ensuring that the cost of opening charging stations and installing charging outlets does not exceed the budget for that year. Constraints (33) both enforce a maximum number of charging outlets at each station and also ensures that the one-time cost to open charging stations is paid. Constraints (34) prevent removing charging outlets and constraints (35) prevent closing charging stations from one year to the next. Constraints (36) set the number of EVs at the start of one year as the number at the end of the previous year. Constraints (37) find the segment of the growth function that the current EV population is in. Constraints (38) ensure that only one segment of the growth function is selected. Constraints (39) cap the the number of EVs by the end of the year by following the growth function. Constraints (40) ensure that the total number of EVs does not decrease from year to year. Constraints (41) are capacity constraints, ensuring that potential new EV users will only decide to purchase an EV if there exists sufficient charging infrastructure.

Parameter	Value
T	4
$ N $	317
$ M $	10
$ N_j $	Varies
e_j (all stations)	6
r	181624
l_j (all stations)	0
c^U (all stations)	50
c_j^F (all stations)	100
B^t (per year)	400
α	0.566
a^t (all years)	$+\infty$
$ S $	5
q^{s-1}, q^s	Varies
m^s	Varies
o^s	Varies

Table 8: Growth Function parameter values

B.2 Generating the Growth Function

The growth function in the Growth Function model gives the number of EVs in the current year as a function of the number of EVs in the previous year. In the absence of the capacity constraints (41), the growth function would directly dictate the number of EVs each year via Constraints (36). We can ensure that the EV growth remains comparable between the Maximum Covering and Growth Function models by using the output from the Maximum Covering model to create the growth function.

More specifically, we assume there are no EV owners at the start of the optimisation period. While this is not a realistic assumption, it ensures feasibility in the Growth Function model. Given a candidate solution (\mathbf{x}, \mathbf{y}) , we run the Maximum Covering model with the desired user classes and parameters over the 20 instances in each dataset. In each instance and for $1 \leq t \leq T$ we calculate the number of users who are covered by \mathbf{x} (given by $\sum_{i \in N} \sum_{r=1}^{R_i} \frac{N_i^t}{R_i} w_i^{rt}$). To calculate the total number of EVs, we add the new EVs in each year to the EVs from the previous year (or the starting EVs in the case of the first year). We take the average result over all instances for each year as our desired growth function, which mimics perfectly the EV growth from the Maximum Covering model.

After normalising for the population—which gives the percentage of the population with EVs in the following year given the percentage of the population with EVs in the current year—, we extend the growth function to cover the entire $[0, 1]$ domain. Both of these steps allow the growth function to be used regardless of population. An example of the normalised,

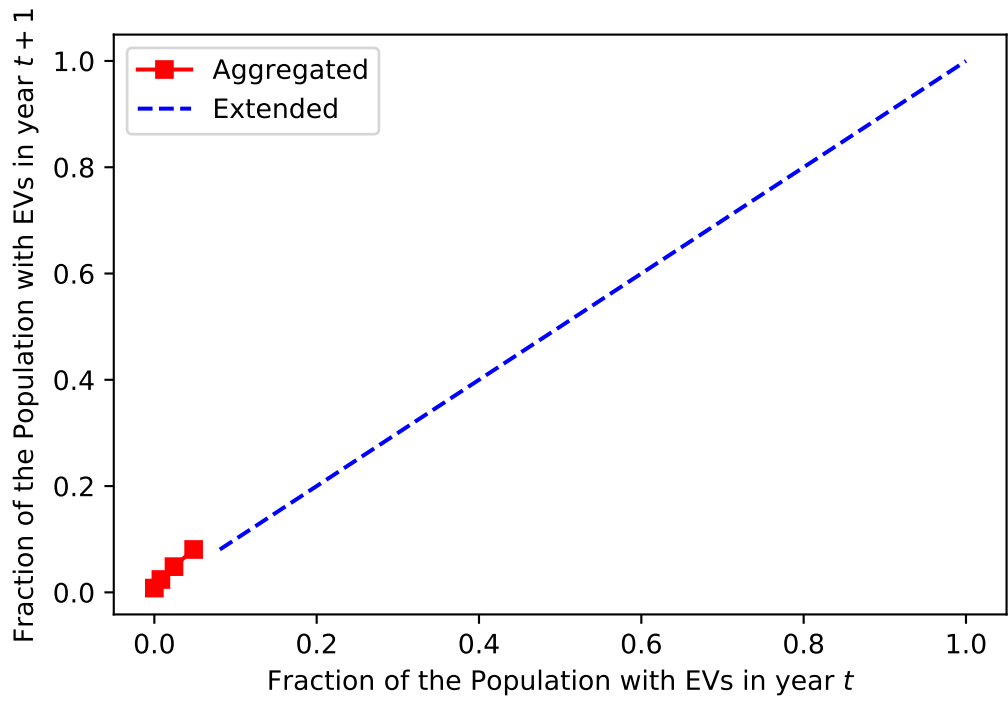


Figure 7: Growth Function Example

extended growth function is given in Figure 7.